CONDENSED MATTER PHYSICS

Original article
DOI: https://doi.org/10.18721/JPM.18301

CRITICAL SCATTERING OF SYNCHROTRON RADIATION IN THE LEAD ZIRCONATE-TITANATE (PZT2.4) USING THE LAST MODEL FOR THE SOFT MODE

S. B. Vakhrushev[1,2,3], *S. A. Reimers*[2,3]✉, *Iu. A. Bronwald*[1]

[1] Ioffe Institute, St. Petersburg, Russia;

[2] Peter the Great St. Petersburg Polytechnic University, St. Petersburg, Russia;

[3] Pacific National University, Khabarovsk, Russia

✉ serafim.reimers@yandex.ru

Abstract. In this work, an experimental and theoretical studies of critical scattering for the $PbZr_{0.976}Ti_{0.024}O_3$ (PZT2.4) compound in the vicinity of the Brillouin zone center have been carried out taking into account the mode coupling. The scattering measurements were carried out at the European Synchrotron Radiation Facility (ESRF). One-dimensional profiles of the scattering intensity dependence on the wave vector were obtained using specially developed programs. The Last model was used for the optical soft mode in the Brillouin zone center. The frequencies and polarization vectors of the renormalized modes were determined by quantitative analysis of the scattering profile for the soft direction [1 0 1]. Good agreement between the calculated results of the model and the experimental data was achieved. The polarization vector's change of the lowest transverse acoustic mode was traced as a function of the reduced wave vector.

Keywords: ferroelectric, antiferroelectric, phase transition, lattice dynamics, critical scattering

Funding: The research was supported by the Ministry of Science and Higher Education of the Russian Federation (Project No. FEME-2024-0005).

C**itation:** Vakhrushev S. B., Reimers S. A., Bronwald Iu. A., Critical scattering of synchrotron radiation in the lead zirconate-titanate (PZT2.4) using the Last model for the soft mode, St. Petersburg State Polytechnical University Journal. Physics and Mathematics. 18 (3) (2025) 9–19. DOI: https://doi.org/10.18721/JPM.18301

Научная статья
УДК 538.913
DOI: https://doi.org/10.18721/JPM.18301

КРИТИЧЕСКОЕ РАССЕЯНИЕ СИНХРОТРОННОГО ИЗЛУЧЕНИЯ В ЦИРКОНАТЕ-ТИТАНАТЕ СВИНЦА (PZT2.4) С ИСПОЛЬЗОВАНИЕМ МОДЕЛИ ЛАСТА ДЛЯ МЯГКОЙ МОДЫ

С. Б. Вахрушев[1,2,3], *С. А. Реймерс*[2,3]✉, *Ю. А. Бронвальд*[1]

[1] Физико-технический институт им. А. Ф. Иоффе РАН, Санкт-Петербург, Россия;

[2] Санкт-Петербургский политехнический университет Петра Великого, Санкт-Петербург, Россия;

[3] Тихоокеанский государственный университет, г. Хабаровск, Россия

✉ serafim.reimers@yandex.ru

Аннотация. В работе проведено экспериментальное и теоретическое исследование критического рассеяния для соединения $PbZr_{0,976}Ti_{0,024}O_3$ (PZT2.4), в окрестности центра зоны Бриллюэна с учетом межмодового взаимодействия. Измерение рассеяния проводилось на Европейском источнике синхротронного излучения (ESRF). Одномерные профили зависимости интенсивности рассеяния от волнового вектора были получены с использованием специально разработанных программ. Для оптической мягкой моды в центре зоны Бриллюэна была использована модель Ласта. Путем количественного анализа профиля рассеяния для мягкого направления [1 0 1] определены частоты и векторы поляризации перенормированных мод. Достигнуто хорошее согласие модельного расчета с экспериментальными данными. Прослежено изменение вектора поляризации низшей поперечной акустической моды как функции приведенного волнового вектора.

Ключевые слова: сегнетоэлектрик, антисегнетоэлектрик, фазовый переход, динамика решетки, критическое рассеяние

Финансирование: Работа выполнена при финансовой поддержке Министерства науки и высшего образования Российской Федерации (проект № FEME-2024-0005).

Ссылка для цитирования: Вахрушев С. Б., Реймерс С. А., Бронвальд Ю. А. Критическое рассеяние синхротронного излучения в цирконате-титанате свинца (PZT2.4) с использованием модели Ласта для мягкой моды // Научно-технические ведомости СПбГПУ. Физико-математические науки. 2025. Т. 18. № 3. С. 9–19. DOI: https://doi.org/10.18721/JPM.18301

Introduction

Comprehensive analysis of X-ray or neutron diffraction patterns of any crystal, even the most perfect ones, shows a diffuse component consisting of some streaks, spots or halos around the main reflections in addition to the sharp Bragg peaks. This background component is commonly known as diffuse scattering. It provides valuable data about the inherently present static or dynamic disorder. Lonsdale and Smith [1] described the very first observations of diffuse scattering in the early 20th century.

There are many excellent books and reviews on the general aspects of diffuse scattering and its application to analysis of diverse physical problems. The most common type of such scattering is thermal diffuse scattering (TDS) by crystal lattice vibrations [2, 3]. The TDS intensity I can be described by the following expression:

$$I_{\mathrm{TDS}}(\mathbf{Q}) = I_0 \sum_{\lambda} \frac{1}{\omega_{\lambda}^2(\mathbf{q})} \left|F_{\lambda}(\mathbf{Q},\mathbf{q})\right|^2 \delta(\mathbf{Q}-\mathbf{q}-\boldsymbol{\tau}), \quad (1)$$

where $\mathbf{Q}$ is the scattering vector; $\mathbf{q} = \mathbf{Q} - \boldsymbol{\tau}$ is the reduced wave vector; $\boldsymbol{\tau}$ is the reciprocal lattice vector; ω_λ is the frequency of mode λ; $F_\lambda(\mathbf{Q},\mathbf{q})$ is the inelastic structure factor.

The factor $F_\lambda(\mathbf{Q},\mathbf{q})$ is determined by the crystal structure (the position r_μ of the atoms in the unit cell) and the polarization vectors of the phonon modes $\mathbf{e}_\mu^\lambda(\mathbf{q})$:

$$F_\lambda(\mathbf{Q},\mathbf{q}) = \sum_\mu \frac{f_\mu(\mathbf{Q})}{\sqrt{2M_\mu}} e^{-W_\mu(\mathbf{Q})} e^{i\mathbf{Q}\cdot\mathbf{r}_i} (\mathbf{Q}\cdot\mathbf{e}_\mu^\lambda(\mathbf{q})), \tag{2}$$

where M_μ is the atomic mass; $e^{-W\mu(\mathbf{Q})}$ is the Debye–Waller factor; $\mathbf{r}_\mu$ is the position of atom μ in the unit cell; $\mathbf{e}_\mu^\lambda(\mathbf{q})$ is the phonon eigenvector for wave vector $\mathbf{q}$ and mode λ, corresponding to atom μ; $f_\mu(\mathbf{Q})$ is the atomic form factor.

It follows from Eq. (1) that TDS by acoustic phonons should be observed in the vicinity of Bragg peaks in all crystals. The frequency of acoustic phonons with small reduced wave vectors is proportional to the magnitude of q. Thus, TDS intensity is inversely proportional to q^2 and the anisotropy is determined by the anisotropy of the sound velocity.

Another important type of TDS is critical scattering by fluctuations in the order parameter in crystals undergoing a phase transition. Critical scattering can be localized around different points of the Brillouin zone, and this localization depends on the symmetry of the order parameter.

Critical scattering in ferroelectrics is of particular interest to us and we intend to focus on it closely in the paper. Apparently, this type of scattering in ferroelectrics was described for the first time in [4]. Similar to the case of diffuse scattering by acoustic phonons, critical scattering in ferroelectrics is concentrated in the vicinity of the Brillouin zone center.

One of the characteristics of critical scattering in intrinsic ferroelectrics is significant suppression of the longitudinal scattering component. This phenomenon was first discovered in [5]. In the case of a cubic isotropic ferroelectric, the expression for the intensity of critical scattering in the paraelectric phase takes the form

$$I\left(\mathbf{Q} = \boldsymbol{\tau} + \mathbf{q}\right) = \frac{I_0 \kappa^2 \sin^2\left(\hat{\mathbf{Q},\mathbf{q}}\right)}{q^2 + \kappa^2}, \tag{3}$$

where I_0 is the peak scattering intensity at $\mathbf{q} = 0$, proportional to static susceptibility χ_0; κ^2 is the square of the inverse correlation length of short-range ferroelectric order.

Cross-sections of surfaces with constant diffuse scattering intensity by planes containing the vector $\boldsymbol{\tau}$ yield constant-intensity contours in the form of two tangent circles (lemniscates) with a zero intensity line coinciding with $\boldsymbol{\tau}$. Taking into account cubic anisotropy somewhat complicates the expressions, however, the intensity remains equal to zero in the case of $\mathbf{q} \parallel \boldsymbol{\tau}$.

Thus, diffuse scattering in the paraelectric phase in the vicinity of the Brillouin zone center includes two components: thermal diffuse scattering by acoustic phonons and critical scattering from the soft mode. Analysis of the data for the vicinities of several nodes of the reciprocal lattice allows to separate these components.

However, the problem becomes significantly more complicated in the presence of mode coupling between transverse optical and acoustic modes. The problem of mode coupling in ferroelectric perovskites was theoretically analyzed in detail in [6–8]. It was found that this coupling leads to significant renormalization of phonon frequencies at $\mathbf{q} \neq 0$ and mixing of polarization vectors of these modes. The Vaks model was applied in [9] to analyze the phonon spectra of potassium tantalate ($KTaO_3$) and in [10–12] to analyze the critical dynamics in lead zirconate ($PbZrO_3$). Renormalization of phonon mode frequencies was correctly described in all cases. As for the mixing of polarization vectors in these papers, only general expressions were given for the polarization vectors $\mathbf{v}_{\lambda\mu\alpha}$ (α is the Cartesian coordinate, λ and μ are defined above) of renormalized modes in terms of phonon eigenvectors at $q = 0$, where there is no coupling. However, their specific type was not determined due to the uncertainty of the eigenvector for soft mode. The diffuse scattering patterns given in [10–12] can only be regarded as qualitative, since they take into account only the directions of ion displacements.

Our paper analyzes diffuse scattering in a solid solution of lead zirconate titanate $PbZr_{0.976}Ti_{0.024}O_3$ (PZT2.4) using the Last model to describe the eigenvector of the soft mode.

Experimental

The measurements were carried out for a sample measuring approximately 1.00 × 0.05 × 0.05 mm, cut from a single crystal of PZT2.4 solid solution grown at the Southern Federal University using the technology described in [13]. The sample was ground and etched in boiling hydrochloric acid to remove the damaged surface layer.

The experiment was conducted using the equipment of the European Synchrotron Radiation Facility (ESRF). The needle-like sample was mounted into a special holder. The holder had the angular range of 150°, allowing to cover a large volume of the reciprocal space. The sample was placed in a nitrogen flux to control its temperature. The wavelength of incident radiation was 0.95 E. A low-noise Pilatus 2M detector was used; the distance from the sample to the detector was 135 mm. The measurements were carried out both under cooling and under heating with a temperature step of 1 °C over a range from 30 to 300 °C.

Software tools developed in MatLab and Java were used to construct one-dimensional profiles of the dependence of scattering intensity on the wave vector. Such diffuse scattering profiles were obtained from a three-dimensional intensity distribution by voxelization. Instead of traditional cubic voxels, we used a voxel that was a straight circular cylinder whose axis coincides with the direction of the profile. Varying the parameters of the cylindrical voxel, we selected its optimal size providing the necessary statistics: a sufficient number of primary detector pixels inside the voxel and the resolution of the wave vector **q**. The voxel radius was 0.2 r.l.u. (reciprocal lattice unit equal to $2\pi/a$), the step was 0.1 r.l.u.

Vaks model with calculation of eigenvectors

We adopted the hypothesis that diffuse scattering is associated with the lowest phonon modes. As shown in [6, 7, 9], calculation and analysis of the corresponding lattice dynamics are simplified in the long-wavelength limit if high-energy optical modes are neglected; in this case, the latter do not give a significant contribution to diffuse scattering. The resulting simplified Hamiltonian takes into account only five modes: three acoustic (2TA (transverse) + LA (longitudinal)) and two low-energy transverse optical (2TO).

The simplified Hamiltonian has the following form:

$$H^{(5)} = \frac{1}{2}\sum_{q}\left[\dot{\mathbf{u}}_{-q}\dot{\mathbf{u}}_{q} + \mathbf{u}_{-q}\hat{A}(\mathbf{q})\mathbf{u}_{q} + \dot{\mathbf{x}}_{-q}\dot{\mathbf{x}}_{q} + \lambda\mathbf{x}_{-q}\mathbf{x}_{q} + \mathbf{x}_{-q}\hat{S}(\mathbf{q})\mathbf{x}_{q} + 2\mathbf{u}_{-q}\hat{V}(\mathbf{q})\mathbf{x}_{q}\right], \quad (4)$$

where u_1, u_2, u_3 and x_1, x_2 (components of vectors **u** and **x**) are the normal coordinates for modes 2TA + LA and 2TO in the reference frame ($X'Y'Z'$), with the Z'-axis parallel to the reduced wave vector **q**, respectively; B, $\hat{S}$, $\hat{V}$ are tensors.

These tensors describe the contribution of short-range interactions and can be written as

$$\hat{A}(\mathbf{q}) = q^2\left(A_a g^a + A_l g^l + A_t g^t\right), \quad (5)$$

$$\hat{S}(\mathbf{q}) = q^2\left(S_a g^a + S_t g^t\right), \quad (6)$$

$$\hat{V}(\mathbf{q}) = q^2\left(V_a g^a + V_t g^t\right), \quad (7)$$

where $g^t_{\alpha\beta} = \delta_{\alpha\beta} - n_\alpha n_\beta$; $g^l_{\alpha\beta} = n_\alpha n_\beta$; $g^a_{\alpha\beta} = \gamma_{\alpha\beta\gamma\delta} n_\gamma n_\delta$.

In this equation, $\mathbf{n} = \mathbf{q}/q$ is a unit vector in the direction of **q**; $\gamma_{\alpha\beta\gamma\delta}$ is a tensor invariant with respect to the symmetry operations of a cubic point group such that

$$\gamma_{\alpha\beta\gamma\delta} = 1 \text{ for } \alpha = \beta = \gamma = \delta \text{ and } \gamma_{\alpha\beta\gamma\delta} = 0 \text{ in all other cases.}$$

The tensor $B(\mathbf{q})$ defines the speed of sound and can be determined from the elastic modulus C, the tensor $\hat{S}(\mathbf{q})$ defines the curvature of the transverse optical mode and the tensor $\hat{V}(\mathbf{q})$ defines the constant of interaction between acoustic and optical branches.

The five-mode Hamiltonian was represented as the sum of isotropic and anisotropic components:

$$H^{(5)}(\mathbf{q}) = H_{is}\left(|q|, \lambda, S_t, A_t, V_t, A_l\right) + H_{anis}\left(\mathbf{q}, S_a, A_a, V_a\right), \quad (8)$$

$$H_{is} = \begin{pmatrix} \lambda + S_t q^2 & 0 & V_t q^2 & 0 & 0 \\ 0 & \lambda + S_t q^2 & 0 & V_t q^2 & 0 \\ V_t q^2 & 0 & A_t q^2 & 0 & 0 \\ 0 & V_t q^2 & 0 & A_t q^2 & 0 \\ 0 & 0 & 0 & 0 & A_l q^2 \end{pmatrix}, \tag{9}$$

$$H_{anis} = q^2 \begin{pmatrix} S_a h_{11} & S_a h_{12} & V_a h_{11} & V_a h_{12} & V_a h_{13} \\ S_a h_{12} & S_a h_{22} & V_a h_{12} & V_a h_{22} & V_a h_{23} \\ V_a h_{11} & V_a h_{12} & A_a h_{11} & A_a h_{12} & A_a h_{13} \\ V_a h_{12} & V_a h_{22} & A_a h_{12} & A_a h_{22} & A_a h_{23} \\ V_a h_{13} & V_a h_{23} & A_a h_{13} & A_a h_{23} & A_a h_{33} \end{pmatrix}, \tag{10}$$

where

$$h_{11} = \frac{2n_2^2 n_3^2}{n_\perp^2},\ h_{12} = \frac{(n_1 n_2 n_3)}{n_\perp^2}(n_3^2 - n_2^2),$$

$$h_{22} = 2n_1^2 \left(n_\perp^2 - \frac{n_2^2 n_3^2}{n_\perp^2} \right),\ h_{13} = \frac{n_2 n_3}{n_\perp}\left(n_2^2 - n_3^2 \right),$$

$$h_{33} = n_1^4 + n_2^4 + n_3^4,\ h_{23} = \frac{n_1}{n_\perp}\left(n_1^2 n_\perp^2 - n_2^4 - n_3^4 \right),$$

$$n_\perp^2 = n_2^2 + n_3^2,$$

Diagonalization of the Hamiltonian $H^{(5)}(\mathbf{q})$ allows to obtain a set of frequencies $\omega_\lambda(\mathbf{q})$ of renormalized modes and a matrix of polarization vectors $D_\lambda(\mathbf{q})$ expressed in terms of the eigenvectors of uncoupled modes in the $X'Y'Z'$ coordinate system considered above. As a first approximation of the eigenvectors, we can select the polarization vectors of phonon modes in the center of the Brillouin zone $V_{\mu a}^{\lambda_0}$ (λ_0 is the number of non-renormalized phonon branch, μ is the number of the atom in the unit cell, α is the Cartesian coordinate).

We use the following numbering of atoms in the cell:

1 for Pb, $\mathbf{r}_1$ = (0 0 0); 2 for Zr (Ti), $\mathbf{r}_2$ = (½ ½ ½); 3 for O_I, $\mathbf{r}_3$ = (½ 0 ½);

4 for O_{II}, $\mathbf{r}_4$ = (0 ½ ½); 5 for O_{III}, $\mathbf{r}_5$ = (½ ½ 0). $\mathbf{r}_i$ is the coordinate of the ith atom in the cell in fractions of the lattice parameter a= 4.6 Å.

The matrix $D_{\lambda j}$ can be transformed into a three-dimensional array of eigenvectors $p_{\nu\lambda\alpha}$ in the Cartesian coordinate system if the metric matrix $M(\mathbf{n})$ is used [9]:

$$M(\mathbf{n}) = \begin{pmatrix} 0 & n_\perp & n_1 \\ -\dfrac{n_3}{n_\perp} & -\dfrac{n_1 n_2}{n_\perp} & n_2 \\ \dfrac{n_2}{n_\perp} & -\dfrac{n_1 n_3}{n_\perp} & n_3 \end{pmatrix}, \tag{11}$$

$$\begin{aligned} pv_{\text{ë1á}} &= M \times D_{\text{ë},j},\ j = 3,4,5, \\ pv_{\text{ë2á}} &= M \times (D_{\text{ë},j}, 0),\ j = 1,2, \end{aligned} \tag{12}$$

The case $l = 1$ corresponds to the contribution of non-renormalized acoustic phonons and $l = 2$ corresponds to the contribution of non-renormalized optical phonons.

Let us introduce the eigenvector matrices $e^{(1)}_{\alpha\mu}$ and $e^{(2)}_{\alpha\mu}$ which are the partial contributions of the atom μ to the displacements corresponding to the acoustic and optical modes, respectively. The index $\alpha = 1, 2, 3$ determines the direction of the displacements.

The values of the elements $e^{(1)}_{\alpha\mu}$ can be determined from the condition that the displacements of all atoms in the cell be equal [14]:

$$u_{\alpha\mu} = \frac{e^{(1)}_{\alpha\mu}}{\sqrt{m_\mu}} = \text{const.} \tag{13}$$

Such a priori definition of $e^{(2)}_{\alpha\mu}$ is impossible for a soft optical mode. The irreducible representation Γ_{15} enters the mechanical representation for the perovskite structure four times, so accordingly, three optical modes of this symmetry should be observed. The Ewald mode, the Last mode, and the Axe mode are often chosen as such modes with mutually orthogonal polarization vectors [15]. It is typically assumed that the soft mode for lead-containing ferroelectrics with a rhombohedral structure is the Last mode. It is also assumed that the Pb^{2+} cation is displaced relative to the group of ions formed by the oxygen octahedron and the central cation.

To simplify the problem, we use the diatomic approximation, assuming that the optical mode can be described if the above group is regarded as a virtual A2 cation.

For the acoustic mode, we can write the following representation without loss of generality:

$$e^{(1)}_{\alpha\mu} = \begin{pmatrix} \sqrt{m_{\text{Pb}}} & \sqrt{m_{\text{A2}}} & \sqrt{m_{\text{A2}}} & \sqrt{m_{\text{A2}}} & \sqrt{m_{\text{A2}}} \\ \sqrt{m_{\text{Pb}}} & \sqrt{m_{\text{A2}}} & \sqrt{m_{\text{A2}}} & \sqrt{m_{\text{A2}}} & \sqrt{m_{\text{A2}}} \\ \sqrt{m_{\text{Pb}}} & \sqrt{m_{\text{A2}}} & \sqrt{m_{\text{A2}}} & \sqrt{m_{\text{A2}}} & \sqrt{m_{\text{A2}}} \end{pmatrix} CC_1. \tag{14}$$

with the normalizing coefficient

$$CC_1 = \sqrt{m_{\text{Pb}} + 4m_{\text{A2}}},$$

where m_{Pb} is the mass of the Pb^{2+} cation, m_{A2} is the sum of the masses of all ions included in the virtual A2 ion.

Evidently,

$$u_{\alpha\mu} = \frac{e^{(1)}_{\alpha\mu}}{\sqrt{m_\mu}} = \text{const.}$$

For the optical mode, taking into account the constancy of the center of mass, we obtain:

$$e^{(2)}_{\alpha\mu} = \begin{pmatrix} -\sqrt{m_{\text{A2}}/m_{\text{Pb}}} & 1/4 & 1/4 & 1/4 & 1/4 \\ -\sqrt{m_{\text{A2}}/m_{\text{Pb}}} & 1/4 & 1/4 & 1/4 & 1/4 \\ -\sqrt{m_{\text{A2}}/m_{\text{Pb}}} & 1/4 & 1/4 & 1/4 & 1/4 \end{pmatrix} CC_2 \tag{15}$$

with the normalizing coefficient $CC_2 = \sqrt{m_{\text{A2}}/m_{\text{Pb}} + 1/4}$.

Indeed, the displacement of the center of mass turns out to equal zero:

$$\frac{\left(\sqrt{m_{A2}/m_{Pb}}\right)m_{Pb}}{\sqrt{m_{Pb}}} - 4\frac{1}{4}\frac{m_{A2}}{\sqrt{m_{A2}}} = \sqrt{m_{A2}} - \sqrt{m_{A2}} = 0. \tag{16}$$

We build an array of 5 × 5 × 3 eigenvectors (number of modes × number of atoms × 3 coordinates) $v_{\lambda\mu\alpha}$:

$$v_{\lambda\mu\alpha} = pv_{\lambda 1\alpha} \times e^{(1)}_{\alpha\mu} + pv_{\lambda 2\alpha} \times e^{(2)}_{\alpha\mu}. \tag{17}$$

Then we can write the following expression for the structure factor of the mode λ:

$$\begin{aligned} F_\lambda(\mathbf{Q},\mathbf{q}) = {} & \frac{f_{Pb}}{\sqrt{m_{Pb}}} e^{i\mathbf{Q}\mathbf{r}_1}\left(\sum_{\alpha=1..3}\left(Q_\alpha v_{\lambda 1\alpha}\right)\right) + \\ & + \frac{1}{\sqrt{m_{A2}}}\left\{ f_{Zr} e^{i\mathbf{Q}\mathbf{r}_2}\left(\sum_{\alpha=1..3}\left(Q_\alpha v_{\lambda 2\alpha}\right)\right) + f_O\left[e^{i\mathbf{Q}\mathbf{r}_3}\left(\sum_{\alpha=1..3}\left(Q_\alpha v_{\lambda 3\alpha}\right)\right) + \right.\right. \\ & \left.\left. + e^{i\mathbf{Q}\mathbf{r}_4}\left(\sum_{\alpha=1..3}\left(Q_\alpha v_{\lambda 4\alpha}\right)\right) + e^{i\mathbf{Q}\mathbf{r}_5}\left(\sum_{\alpha=1..3}\left(Q_\alpha v_{\lambda 5\alpha}\right)\right)\right]\right\}. \end{aligned} \tag{18}$$

The values of the atomic scattering factors are calculated by the formulas given in [16].

Analysis of experimental data

We analyzed one-dimensional scans along the [1 0 1] direction through the reciprocal lattice nodes (1 0 −1) and (0 0 3). The diffuse scattering intensity at point **Q** was calculated as follows:

$$I(\mathbf{Q}) = I_0 \sum_{\lambda=1}^{5} F_\lambda^2(\mathbf{Q},\mathbf{q}) \frac{1}{\omega_\lambda^2(\mathbf{q})} + \text{Bck}, \tag{19}$$

where $\omega_\lambda^2(\mathbf{q})$ is the square of the frequency of the renormalized mode λ, equal to λth eigenvalue of the Hamiltonian $H^{(5)}(\mathbf{q})$; the expression $F_\lambda^2(\mathbf{Q},\mathbf{q})$ is calculated by Eq. (18); I_0 is the scale factor; the term Bck is the background.

Parameters A_l, A_t, A_a, S_t, S_a (in (meV)^2/(r.l.u.)^2) were assumed to be equal to the values for pure lead zirconate, given in [12]:

$$A_l = 2508,\ A_t = 879,\ A_a = -111,\ S_t = 1800,\ S_a = -610.$$

The results were processed in two stages. At the first stage, the parameters V_t, ω_0^2, the scale multiplier and background were fitted for the node (1 0 −1). Since the experimental data for different nodes were normalized differently, only the scale factor and background were fitted for node (0 0 3) and the remaining parameters were taken from the fit for node (1 0 −1).

Experimental data in Fig. 1 are shown by dots and their statistical errors are shown by vertical bars. The central region $-0.05 \le q \le 0.05$ to which Bragg scattering makes a contribution was excluded from the fit. It can be seen that the calculated curves completely coincide with the experimental ones within the limits of statistical errors.

As a result of the fitting, we obtained the following parameter values:

$$V_t = 1073\ (\text{meV})^2/(\text{r.l.u.})^2,\ \omega^2{}_0 = 4.58\ (\text{meV})^2.$$

For comparison, we calculated the diffuse scattering intensity without taking into account the polarization vectors (red dashed lines in Fig. 1). In this case, the dependence $\omega_\lambda^2(\mathbf{q})$ and directions of atomic displacements $pv_{\lambda l\alpha}$ (12) were used.

For acoustic phonons, taking into account expression (18), we can write an expression for structure factors at $q = 0$ ($\mathbf{Q} = \boldsymbol{\tau}$):

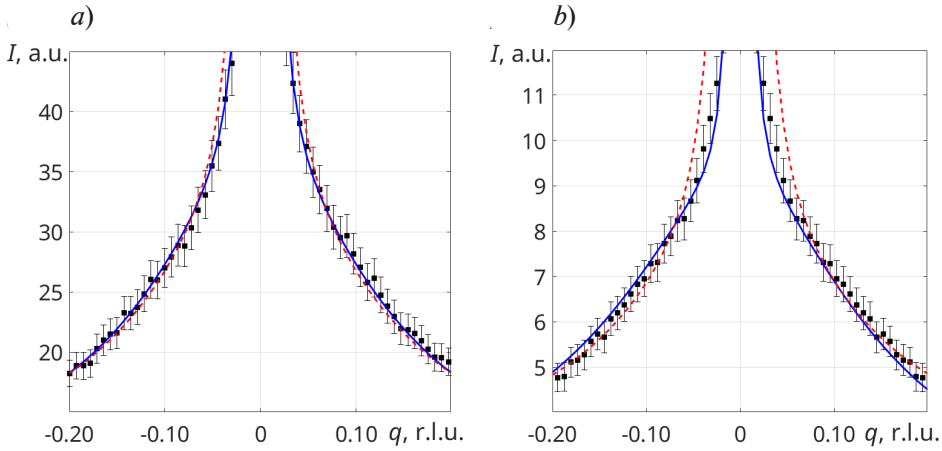

Fig. 1. Experimental (points) and calculated (lines) dependences of diffuse scattering intensity I on reduced wave vector **q** for two scattering vectors: **Q** = (1 + q, 0, −1 + q) (a) and (q, q, 3) (b) Calculated data were obtained using polarization vectors (blue solid lines) and taking into account only the type of dispersion curves and the direction of displacements (red dashed lines). The statistical errors of the experiment are shown by vertical bars

$$F \sim f_{\mathrm{Pb}} + f_{\mathrm{Zr}} \cos(\pi(h+k+l)) + \\ + f_{\mathrm{o}}(\cos(\pi(h+k)) + \cos(\pi(h+k))\cos(\pi(h+k))). \tag{20}$$

Therefore,

$$F_{(1\,0\,-1)} \sim f_{\mathrm{Pb}} + f_{\mathrm{Zr}} - f_{\mathrm{O}}, \\ F_{(0\,0\,3)} \sim f_{\mathrm{Pb}} - f_{\mathrm{Zr}} - f_{\mathrm{O}}. \tag{21}$$

In the case of node (1 0 −1) with the larger structure factor, renormalization of the polarization vectors for acoustic phonons makes a relatively small contribution to intensity, that is, such a simplified calculation gives only qualitative agreement with the experiment (see Fig. 1,*a*).

On the other hand, renormalization of the polarization vectors plays an important role in the case of node (0 0 3) with a small elastic structure factor. It should be noted here that data analysis in the vicinity of several nodes of the reciprocal lattice is required to reliably determine the parameters of the Hamiltonian $H^{(5)}(\mathbf{q})$. The fundamental principles for determining dispersion curves were addressed in [2]. While exact determination of phonon dispersion curves is impossible in the general case, the polarization vectors can be found.

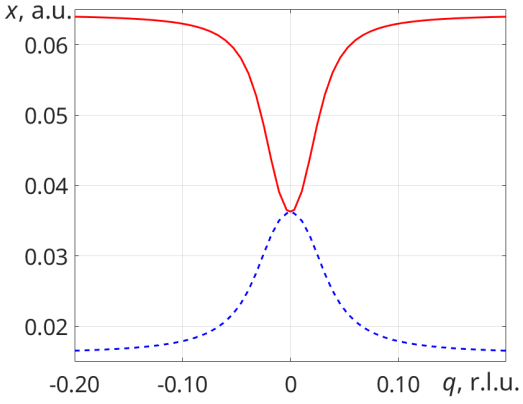

Fig. 2. Dependences of reduced displacements along the x-axis for lead (red solid line) and zirconium (blue dashed line) for the lowest phonon mode

We established the dependency $\nu_{\lambda\mu\alpha}(q)$.

Fig. 2 shows the reduced displacements

$$u^{N}_{\lambda\mu\alpha} = \frac{v_{\lambda\mu\alpha}}{\sqrt{m_{\mu}}}$$

along the x-axis (α = 1) for lead (μ = 1) and zirconium (μ = 2) atoms for the lowest phonon mode (which is transverse acoustic polarized in the (x 0 z) plane). At q = 0, the given displacements are equal, as they should be for acoustic vibrations. As q increases, the contribution of lead displacements increases dramatically. The obtained result is in good agreement with the assumption made in [10] that it is the softening

of the renormalized transverse acoustic phonon branch that causes the transition to the antiferroelectric phase and that this transition is associated with antiparallel displacements of lead ions.

Conclusion

The study develops an approach to quantifying diffuse scattering in the vicinity of the Brillouin zone center in perovskite-like crystals in the presence of mode coupling. Phonon dispersion curves were calculated using the Vaks model. The polarization vectors of renormalized phonon modes were described as a linear combination of eigenvectors of transverse acoustic and optical phonons in the center of the Brillouin zone, where mode coupling is absent. The Last model was used to describe the soft mode associated with the ferroelectric phase transition. This model assumes that the lead cation oscillates relative to a rigid-body group of atoms including an oxygen octahedron and a central cation. The mixing coefficients depending on the reduced wave vector were determined from diagonalization of the five-mode Hamiltonian. The developed approach was used to analyze diffuse scattering in solid solution of the PZT2.4 ferroelectric.

A comparison between the experimental data and the calculations was carried out for the vicinity of the reciprocal lattice nodes (1 0 −1) and (0 0 3). It was confirmed that the proposed formalism provides a good description of the experimental data in both nodes simultaneously.

The approach we proposed and developed allows to efficiently analyze data simultaneously in several Brillouin zones and reliably determine the parameters of the dynamic Hamiltonian. We established the dependence of reduced atomic displacements on the reduced magnitude of the wave vector, confirming the predominant role of renormalization of the acoustic phonon branch for the antiferroelectric transition associated with antiparallel displacements of the lead ion.

REFERENCES

1. **Lonsdale K.Y., Smith H.,** An experimental study of diffuse X-ray reflexion by single crystals, Proc. R. Soc. Lond. A. 179 (976) (1941) 8–50.

2. **Xu R., Chiang T. C.,** Determination of phonon dispersion relations by X-ray thermal diffuse scattering, Z. Kristallogr. Cryst. Mater. 220 (12) (2005) 1009–1016.

3. **Welberry T. R., Weber T.,** One hundred years of diffuse scattering, Crystallogr. Rev. 22 (1) (2016) 2–78.

4. **Comes R., Lambert M., Guinier A.,** Dйsordre linйaire dans les cristaux (cas du silicium, du quartz, et des pйrovskites ferroйlectriques), Acta Cryst. A26 (2) (1970) 244–254.

5. **Cochran W.,** Dynamical, scattering and dielectric properties of ferroelectric crystals, Adv. Phys. 18 (72) (1969) 157–192.

6. **Vaks V. G.,** Vvedenie v mikroskopicheskuyu teoriyu segneto-elektrikov. [Introduction to the microscopic theory of ferroelectrics], Nauka Publishing, Moscow, 1973 (in Russian).

7. **Vaks V. G.,** Phase transitions of the displacement type in ferroelectrics, J. Exp. Theor. Phys. 27 (3) (1968) 486–494.

8. **Axe J. D., Harada J., Shirane G.,** Anomalous acoustic dispersion in centrosymmetric crystals with soft optic phonons, Phys. Rev. B. 1 (3) (1970) 1227–1234.

9. **Farhi E., Tagantsev A. K., Currat R., et al.,** Low energy phonon spectrum and its parameterization in pure $KTaO_3$ below 80 K, Eur. Phys. J. B. 15 (4) (2000) 615–623.

10. **Tagantsev A. K., Vaideeswaran K., Vakhrushev S. B., et al.,** The origin of antiferroelectricity in $PbZrO_3$, Nat. Commun. 4 (1) (2013) 2229–2236.

11. **Burkovsky R. G., Tagantsev A. K., Vaideeswaran K., et al.,** Lattice dynamics and antiferroelectricity in $PbZrO_3$ tested by X-ray and Brillouin light scattering, Phys. Rev. B. 90 (14) (2014) 144301.

12. **Andronikova D. A., Burkovsky R. G., Filimonov A. V., et al.,** Phonon dispersion calculations using the Vaks model in antiferroelectric lead zirconate, J. Adv. Dielectr. 5 (02) (2015) 1550016.

13. **Leontiev N. G., Smotrakov V. G., Fesenko E. G.,** Phase diagram of $PbZr_{1-x}Ti_xO_3$ with $x < 0.1$, Inorg. Mater. 18 (3) (1982) 374.

14. **Sylyom J.,** Fundamentals of the physics of solids, Vol. 1., Springer-Verlag, Inc, Berlin, Heidelberg, 2007.

15. **Harada J., Axe J. D., Shirane G.,** Determination of the normal vibrational displacements in several perovskites by inelastic neutron scattering, Acta Cryst. A26 (6) (1970) 608–612.

16. Graz center of physics. Atomic form factors. http://lampx.tugraz.at/~hadley/ss1/crystaldiffraction/atomicformfactors/formfactors.php. Accessed May 16, 2025.

СПИСОК ЛИТЕРАТУРЫ

1. **Lonsdale K.Y., Smith H.** An experimental study of diffuse X-ray reflexion by single crystals // Proceedings of the Royal Society of London. Series A. 1941. Vol. 179. No. 976. Pp. 8–50.

2. **Xu R., Chiang T. C.** Determination of phonon dispersion relations by X-ray thermal diffuse scattering // Zeitschrift fьr Kristallographie-Crystalline Materials. 2005. Vol. 220. No. 12. Pp. 1009–1016.

3. **Welberry T. R., Weber T.** One hundred 2025s of diffuse scattering // Crystallography Reviews. 2016. Vol. 22. No. 1. Pp. 2–78.

4. **Comes R., Lambert M., Guinier A.** Dйsordre linйaire dans les cristaux (cas du silicium, du quartz, et des pйrovskites ferroйlectriques) // Acta Crystallographica. Section A: Foundations and Advances. 1970. Vol. A26. Part 2. Pp. 244–254.

5. **Cochran W.** Dynamical, scattering and dielectric properties of ferroelectric crystals // Advances in Physics. 1969. Vol. 18. No. 72. Pp. 157–192.

6. **Вакс В. Г.** Введение в микроскопическую теорию сегнетоэлектриков. М.: Наука, 1973. 327 с.

7. **Вакс В. Г.** О фазовых переходах типа смещения в сегнетоэлектриках // Журнал экспериментальной и теоретической физики. 1968. Т. 54. № 3. С. 910–926.

8. **Axe J. D., Harada J., Shirane G.** Anomalous acoustic dispersion in centrosymmetric crystals with soft optic phonons // Physical Review B. 1970. Vol. 1. No. 3. Pp. 1227–1234.

9. **Farhi E., Tagantsev A. K., Currat R., Hehlen B., Courtens E., Boatner L. A.** Low energy phonon spectrum and its parameterization in pure $KTaO_3$ below 80 K // The European Physical Journal B. 2000. Vol. 15. No. 4. Pp. 615–623.

10. **Tagantsev A. K., Vaideeswaran K., Vakhrushev S. B., et al.** The origin of antiferroelectricity in $PbZrO_3$ // Nature Communications. 2013. Vol. 4. No. 1. Pp. 2229–2236.

11. **Burkovsky R. G., Tagantsev A. K., Vaideeswaran K., et al.** Lattice dynamics and antiferroelectricity in $PbZrO_3$ tested by X-ray and Brillouin light scattering // Physical Review B. 2014. Vol. 90. No. 14. P. 144301.

12. **Andronikova D. A., Burkovsky R. G., Filimonov A. V., Tagantsev A. K., Vakhrushev S. B.** Phonon dispersion calculations using the Vaks model in antiferroelectric lead zirconate // Journal of Advanced Dielectrics. 2015. Vol. 5. No. 02. P. 1550016.

13. **Леонтьев Н. Г., Смотраков В. Г., Фесенко Е. Г.** Фазовая диаграмма $PbZr_{1-x}Ti_xO_3$ при $x <$ 0,1 // Известия Академии наук СССР. Неорганические материалы. 1982. Т. 18. № 3. С. 449–453.

14. **Sylyom J.** Fundamentals of the physics of solids. Vol. 1. Berlin, Heidelberg: Springer-Verlag, Inc, 2007. 697 p.

15. **Harada J., Axe J. D., Shirane G.** Determination of the normal vibrational displacements in several perovskites by inelastic neutron scattering // Acta Crystallographica. Section A: Foundations and Advances. 1970. Vol. A26. Part 6. Pp. 608–612.

16. Graz center of physics. Atomic form factors. Режим доступа: http://lampx.tugraz.at/~hadley/ss1/crystaldiffraction/atomicformfactors/formfactors.php (Дата обращения: 16.05.2025).

THE AUTHORS

VAKHRUSHEV Sergey B.
Ioffe Institute of RAS, St. Petersburg, Russia;
Peter the Great St. Petersburg Polytechnic University, St. Petersburg, Russia;
Pacific National University, Khabarovsk, Russia
26 Polytekhnicheskaya St., St. Petersburg, 194021, Russia
s.vakhrushev@mail.ioffe.ru
ORCID: 0000-0003-4867-1404

REIMERS Serafim A.
Peter the Great St. Petersburg Polytechnic University, St. Petersburg, Russia;
Pacific National University, Khabarovsk, Russia
29 Politekhnicheskaya St., St. Petersburg, 195251, Russia
serafim.reimers@yandex.ru
ORCID: 0009-0009-9951-758X

BRONWALD Iurii A.
Ioffe Institute of RAS
26 Polytekhnicheskaya St., St. Petersburg, 194021, Russia
yuramel@gmail.com
ORCID: 0000-0003-0225-0487

СВЕДЕНИЯ ОБ АВТОРАХ

ВАХРУШЕВ Сергей Борисович – *доктор физико-математических наук, главный научный сотрудник, заведующий лабораторией нейтронных исследований Физико-технического института имени А. Ф. Иоффе РАН, профессор Высшей инженерно-физической школы Санкт-Петербургского политехнического университета Петра Великого; ведущий научный сотрудник Тихоокеанского государственного университета.*
194021, Россия, г. Санкт-Петербург, Политехническая ул., 26
s.vakhrushev@mail.ioffe.ru
ORCID: 0000-0003-4867-1404

РЕЙМЕРС Серафим Андреевич – *аспирант Высшей инженерно-физической школы Санкт-Петербургского политехнического университета Петра Великого; младший научный сотрудник Тихоокеанского государственного университета.*
195251, Россия, г. Санкт-Петербург, Политехническая ул., 29
serafim.reimers@yandex.ru
ORCID: 0009-0009-9951-758X

БРОНВАЛЬД Юрий Алексеевич – *научный сотрудник Физико-технического института имени А. Ф. Иоффе РАН.*
194021, Россия, г. Санкт-Петербург, Политехническая ул., 26
yuramel@gmail.com
ORCID: 0000-0003-0225-0487

Received 16.05.2025. Approved after reviewing 29.05.2025. Accepted 29.05.2025.
Статья поступила в редакцию 16.05.2025. Одобрена после рецензирования 29.05.2025. Принята 29.05.2025.